

# Monte-Carlo study of correlations in quantum spin chains at non-zero temperature

 Y.J. Kim<sup>1,2,a</sup>, M. Greven<sup>1,b</sup>, U.-J. Wiese<sup>1</sup>, and R.J. Birgeneau<sup>1</sup>
<sup>1</sup> Department of Physics, Massachusetts Institute of Technology, Cambridge, MA 02139, USA

<sup>2</sup> Division of Engineering and Applied Sciences, Harvard University, Cambridge, MA 02138, USA

Received: 23 December 1997 / Revised and Accepted: 11 March 1998

**Abstract.** Antiferromagnetic Heisenberg spin chains with various spin values ( $S = 1/2, 1, 3/2, 2, 5/2$ ) are studied numerically with the quantum Monte-Carlo method. Effective spin  $S$  chains are realized by ferromagnetically coupling  $n = 2S$  antiferromagnetic spin chains with  $S = 1/2$ . The temperature dependence of the uniform susceptibility, the staggered susceptibility, and the static structure factor peak intensity are computed down to very low temperatures,  $T/J \approx 0.01$ . The correlation length at each temperature is deduced from numerical measurements of the instantaneous spin-spin correlation function. At high temperatures, very good agreement with exact results for the classical spin chain is obtained independent of the value of  $S$ . For the  $S = 2$  chain which has a gap  $\Delta$ , the correlation length and the uniform susceptibility in the temperature range  $\Delta < T < J$  are well predicted by the semi-classical theory of Damle and Sachdev.

**PACS.** 75.10.Jm Quantized spin models – 75.40.Cx Static properties (order parameter, static susceptibility, heat capacities, critical exponents, etc.) – 75.40.Mg Numerical simulation studies

## 1 Introduction

For many years, low-dimensional quantum magnets have drawn much interest from both the theoretical and experimental condensed matter physics communities. Powerful experimental tools like neutron scattering have elucidated the basic physics of two-dimensional (2D) antiferromagnets, such as  $\text{K}_2\text{NiF}_4$  ( $S = 1$ ) [1], and one-dimensional (1D) systems, such as  $(\text{CD}_3)_4\text{NMnCl}_3$  (TMMC) ( $S = 5/2$ ) [2,3]. The discovery of high-temperature superconductivity in 1986 sparked renewed interest in this field, since the parent compounds of these superconductors provide very good realizations of 2D spin-1/2 square-lattice quantum Heisenberg antiferromagnets [4,5]. Recently, quantum spin ladders and spin chains have also attracted much attention, since new copper oxides with such structures have become available; these systems are of intrinsic interest and they also allow one to compare experimental results with the relevant quantum field theories and numerical simulations [6].

We report here a Monte-Carlo study of antiferromagnetic spin chains as a function of spin quantum number  $S$  and temperature  $T$ . Recent advances in computer technology as well as the development of a powerful loop cluster algorithm [7] have made it possible to perform a very

detailed study of various experimentally relevant thermodynamic quantities. In this paper, we compute the  $S$  and  $T$  dependence of the uniform susceptibility,  $\chi_u(S, T)$ ; the spin-spin correlation length,  $\xi(S, T)$ ; the staggered susceptibility,  $\chi_s(S, T)$ ; and the static structure factor at  $q = \pi$ ,  $C_\pi(S, T)$ . There exists a large number of quasi-1D magnetic systems, such as  $\text{Sr}_2\text{CuO}_3$  ( $S = 1/2$ ) [8], copper benzoate ( $S = 1/2$ ) [9],  $\text{Ni}(\text{C}_2\text{H}_8\text{N}_2)_2\text{NO}_2\text{ClO}_4$  ( $S = 1$ ) [10],  $\text{Y}_2\text{BaNiO}_5$  ( $S = 1$ ) [11],  $\text{CsVCl}_3$  ( $S = 3/2$ ) [12],  $(\text{C}_{10}\text{H}_8\text{N}_2)\text{MnCl}_3$  ( $S = 2$ ) [13], and TMMC ( $S = 5/2$ ) [2]. These magnets all exhibit nearly ideal 1D behavior over a considerable range of temperature. Therefore, our study facilitates comparisons among experimental results, numerical simulations, and theories for such materials.

The Hamiltonian for the nearest-neighbor Heisenberg spin chain is

$$\mathcal{H} = J \sum_i \mathbf{S}_i \cdot \mathbf{S}_{i+1}, \quad (1)$$

where  $J$  is positive for an antiferromagnet. We use units in which  $\hbar = k_B = g\mu_B = 1$ . The study of the Hamiltonian (1) has a long history that dates back to the remarkable exact solution found by Bethe in 1931 for  $S = 1/2$  [14]. He found the ground-state eigenfunction for this system and showed that there is no long-range order at  $T = 0$ . In 1962, des Cloizeaux and Pearson [15] derived the exact dispersion relation of the lowest-lying excited states at  $T = 0$ . Luther and Peschel [16] showed that the spectrum is gapless without magnetic ordering in the ground state, and that the spin correlation function

<sup>a</sup> e-mail: ykim@yoko.mit.edu

<sup>b</sup> *Present address:* Department of Applied Physics and Stanford Synchrotron Radiation Laboratory, Stanford University, Stanford, CA 94305, USA.

decays algebraically with distance. Haldane [17] eventually conjectured that half-odd-integer spin chains would behave qualitatively like a  $S = 1/2$  chain, while for integer spin chains the zero-temperature spin correlations would decay exponentially with distance due to the presence of an energy gap,  $\Delta$ , in the excitation spectrum. Both numerical and experimental confirmation of this conjecture followed [18,19]. The low-energy and low-temperature properties of integer spin chains are well described by the 1D quantum  $O(3)$  nonlinear  $\sigma$  model without any topological term [17]. When conformal field theory techniques were applied to 1D quantum systems, it was shown that the integrable  $S = 1/2$  Hamiltonian, at low energies, is equivalent to the  $SU(2)$  Wess-Zumino-Novikov-Witten (WZNW) model with a topological coupling constant  $k = 1$  [20]. Moreover, all half-odd-integer spin- $S$  Heisenberg models were predicted to be equivalent to the  $k = 1$  WZNW model, independent of  $S$  [21,22].

In the limit of classical spins,  $S \rightarrow \infty$ , the Hamiltonian equation (1) was solved exactly by Fisher in 1964 [23]. In order to accommodate the limit  $S \rightarrow \infty$ , equation (1) is conveniently rewritten in terms of the unit vector  $\hat{\mathbf{s}}_i \equiv \mathbf{S}_i / \sqrt{S(S+1)}$ , thus introducing the energy scale  $JS(S+1)$  in place of  $J$ . The results for the correlation length and the uniform susceptibility per spin are, respectively,

$$\frac{\xi(S \rightarrow \infty, T)}{a} = -\frac{1}{\ln u(S, T)} \quad (2)$$

and

$$\chi_u(S \rightarrow \infty, T) = \frac{S(S+1)}{3T} \frac{1 + u(S, T)}{1 - u(S, T)}, \quad (3)$$

where  $a$  is the lattice constant and  $u(S, T)$  is given by

$$u(S, T) = \coth \left[ \frac{JS(S+1)}{T} \right] - \frac{T}{JS(S+1)}.$$

For the experimental system TMMC ( $S = 5/2$ ), the correlation lengths in the Heisenberg regime obtained from neutron scattering could be explained very well by equation (2), without any adjustable parameters, since  $J$  had been determined independently [2].

In Section 2, we give a brief description of our Monte-Carlo method. Uniform susceptibility data are shown and discussed in Section 3, while staggered quantities such as the correlation lengths, staggered susceptibilities, and static structure factor peak intensities are presented in Section 4. The properties of integer spin chains in the context of recent field theory results are discussed in Section 5. A comparison between the results for the spin- $S$  chain and the  $n$ -chain  $S = 1/2$  ladder is also made in Section 5.

## 2 Quantum Monte-Carlo

We have carried out quantum Monte-Carlo simulations on large lattices utilizing the loop cluster algorithm [7]. In

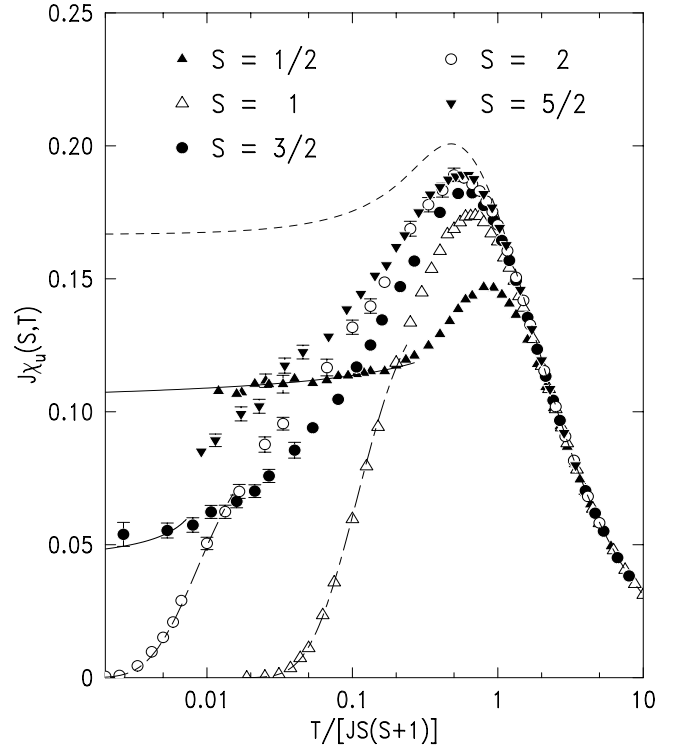


**Fig. 1.** The uniform susceptibility per spin is shown as a function of  $T/[JS(S+1)]$ . The dashed line is a plot of Fisher's result for the classical spin system, equation (3). The dot-dashed lines are fits for  $S = 1$  and  $S = 2$  to equation (4). The solid lines for  $S = 1/2$  and  $S = 3/2$  are the WZNW nonlinear  $\sigma$  model expression, equation (5).

order to realize chains with spin  $S > 1/2$ , an  $n$ -chain spin- $1/2$  ladder with an infinitely strong ferromagnetic inter-chain coupling is mapped to a  $S = n/2$  chain [24]. The same algorithm employed to study spin ladders is used with minor modifications [25]. The lengths and Trotter numbers of the chains are chosen so as to minimize any finite-size and lattice-spacing effects. The chain length is kept at least 10 times larger than the calculated correlation length. Spin states are updated about  $10^4$  times to reach equilibrium and then measured  $10^5$  times. We are able to simulate as many as 100 million lattice points on our workstation.

## 3 Uniform susceptibility

The uniform susceptibility is shown in Figure 1 as a function of  $T/[JS(S+1)]$ . The dashed line is a plot of Fisher's result for the classical spin chain, equation (3). At high temperatures,  $T/[JS(S+1)] > 1$ , the agreement among the results for all the spin values and equation (3) is very good. As predicted by Haldane [17], at low temperatures the uniform susceptibilities of integer spin chains behave markedly differently from those of half-odd-integer spin chains. An exponential activation due to an energy gap is

observed for integer  $S$ . By fitting the uniform susceptibility to the low-temperature expression [26, 27]

$$\chi_u(S, T) = \frac{1}{v} \left( \frac{2\Delta}{\pi T} \right)^{1/2} \exp\left(-\frac{\Delta}{T}\right), \quad (4)$$

where  $\Delta$  is the Haldane gap and  $v$  is the spin-wave velocity, we extract the values  $\Delta_{S=1}/J = 0.40(1)$ ,  $v_{S=1}/Ja = 2.5(1)$ ,  $\Delta_{S=2}/J = 0.090(5)$ , and  $v_{S=2}/Ja = 4.50(33)$ . The uniform susceptibility data are fitted only for  $T < \Delta/2$ , and the results of this analysis agree with the values deduced in previous studies [18, 28–30].

For the  $S = 1/2$  chain, the theoretical low-temperature result for the WZNW nonlinear  $\sigma$  model [31],

$$\chi_u(1/2, T) = \frac{1}{2\pi v} + \frac{1}{4\pi v} \left[ \frac{1}{\ln(T_0/T)} - \frac{\ln(\ln(T_0/T) + 1/2)}{2\ln(T_0/T)^2} \right], \quad (5)$$

is plotted as a solid line. Here the spin-wave velocity  $v_{S=1/2}/Ja = \pi/2$ , and  $T_0/J \approx 1.8$ . The hypothesis that all half-odd-integer Heisenberg chains are in the same universality class as the  $S = 1/2$  chain, namely the  $k = 1$  WZNW model, is now generally accepted. However, this claim was initially considered to be controversial, since integrable spin- $S$  Hamiltonians are equivalent to the WZNW model with  $k = 2S$  [32]. A recent numerical study by Hallberg *et al.* [33] gave strong evidence that  $k = 1$  for the WZNW model of the  $S = 3/2$  chain, thus supporting the above hypothesis. We give here additional evidence in favor of this claim. The asymptotic value of the uniform susceptibility for the  $k = 2S$  WZNW model is different from that of equation (5). Specifically, at  $T \rightarrow 0$ ,  $\chi_u(S, T) \rightarrow S/\pi v_S$  rather than  $\chi_u(S, 0) = 1/2\pi v_S$ . If we use the calculated value  $v_{S=3/2}/Ja = 3.87$  for the spin-wave velocity [33], we obtain  $J\chi_u(3/2, 0) \approx 0.12$  for the  $k = 2S$  model and  $J\chi_u(3/2, 0) \approx 0.04$  for the  $k = 1$  model. Therefore, as is evident from Figure 1, our data for  $S = 3/2$  show clearly that the  $S = 3/2$  Heisenberg chain is equivalent to the WZNW model with  $k = 1$ . We have, in fact, fitted our  $S = 3/2$  chain data for  $\chi_u$  with equation (5). The spin-wave velocity is held fixed at the value given above and only  $T_0$  is adjusted. As may be seen in Figure 1 the fit is very good at low temperatures, as expected. For the  $S = 5/2$  chain, we are not able to obtain numerical data down to low enough temperatures to yield a meaningful test of equation (5).

#### 4 Correlation length, staggered susceptibility, and static structure factor peak intensity

In order to deduce the spin-spin correlation length,  $\xi(S, T)$ , the instantaneous spin-spin correlation function,  $C(r)$ , is computed and fitted to the asymptotic form

$$C(r) \sim \frac{\exp(-r/\xi)}{r^\lambda}. \quad (6)$$

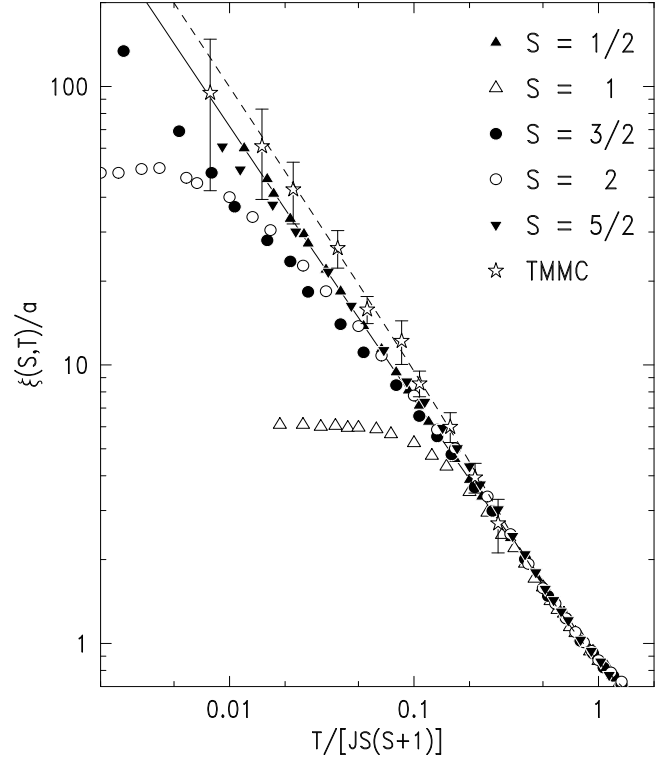


**Fig. 2.** The spin-spin correlation length deduced from fitting the computed correlation function to the asymptotic form, equation (6), is plotted as a function of temperature. Also shown are the correlation lengths of TMMC from reference [2]. The classical spin system result, equation (2), is shown as a dashed line. The solid line is equation (7) for the  $S = 1/2$  chain.

Equation (6) is equivalent to 1D and 2D Ornstein-Zernike (OZ) forms when  $\lambda = 0$  and  $\lambda = 1/2$ , respectively. Only data with  $r > 3\xi$  are included in the fit to ensure that the asymptotic behavior is probed. For half-odd-integer spin chains, the 1D OZ form is found to work very well over the entire temperature range. The spin correlations for integer spin chains, however, are found to go through a crossover with decreasing temperature, from the 1D to the 2D OZ form at  $T \approx \Delta/2$ . Specifically, the 2D OZ form gives a better description of the computed spin correlations at low temperatures. This behavior also was observed previously for spin ladders of even width [25]. The low-temperature correlation function for the  $S = 1$  chain is known to be proportional to the modified Bessel function  $K_0(r/\xi)$  [29];  $K_0$  is also used to fit our integer spin chain data, and the results are consistent with those extracted using equation (6).

In Figure 2, the numerical correlation length is shown together with  $\xi(T)$  for TMMC obtained from neutron scattering experiments [2]. The result for the classical spin system, equation (2), is shown as the dashed line. The agreement among the spin correlation lengths for the different quantum spin chains, and with the classical curve, is very good for temperatures as low as  $T/[JS(S+1)] \approx 0.2$ , which corresponds to  $\xi/a \approx 4$ . As the temperature is

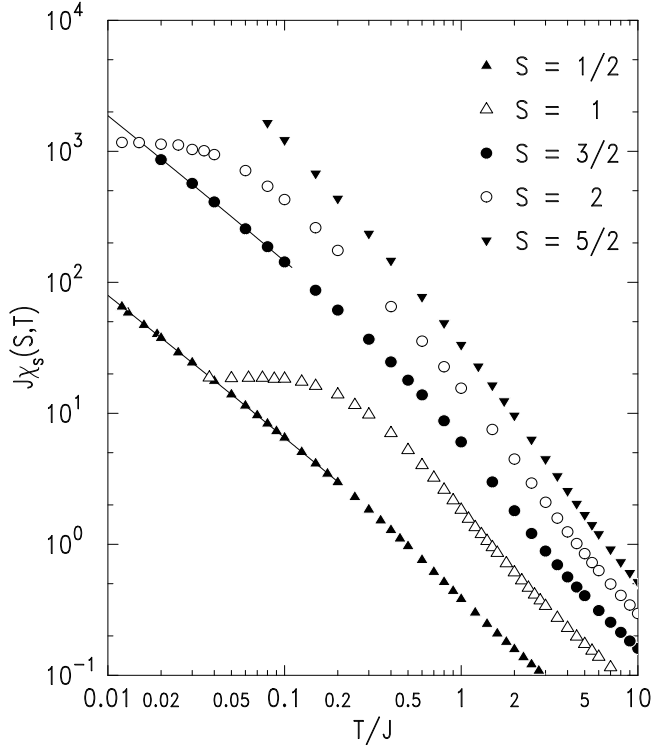


**Fig. 3.** The temperature dependence of the staggered susceptibility per spin. The solid lines are the results of fits to equation (8).

lowered further, the data begin to deviate from the classical curve. Note, that for  $S \geq 1$ , as the spin value is increased, the agreement between the quantum and classical results persists down to progressively lower temperatures. Because of the presence of a gap for integer spin chains,  $\xi(T)$  remains finite as  $T \rightarrow 0$ . We estimate that  $\xi(1, 0)/a = 6.0(1)$  and  $\xi(2, 0)/a = 50(1)$ . These results satisfy the relation  $v = \Delta\xi$  with the values for  $v$  and  $\Delta$  obtained above;  $\Delta_{S=1}/J = 0.40(1)$ ,  $v_{S=1}/Ja = 2.5(1)$ ,  $\Delta_{S=2}/J = 0.090(5)$ , and  $v_{S=2}/Ja = 4.50(33)$ , and also agree with those of previous numerical studies within the combined errors [30,34]. For the  $S = 1/2$  chain, we also plot in Figure 2 the WZNW model prediction,

$$\frac{1}{\xi(1/2, T)} = T \left[ 2 - \frac{1}{\ln(T_0/T)} + \frac{\ln(\ln(T_0/T) + 1/2)}{2 \ln(T_0/T)^2} \right], \quad (7)$$

with the parameters obtained by Nomura and Yamada in a thermal Bethe ansatz study [35].

The staggered susceptibility per spin is shown in Figure 3. The different behaviors of integer and half-odd-integer spin chains are clearly manifest in this plot. In Figure 4, the static structure factor  $C_q$  at  $q = \pi$  is plotted as a function of temperature. Note, that for integer spin chains  $C_\pi(S, T)$  peaks at  $T \approx \Delta/2$ ; closely similar behavior is observed for spin-1/2 ladders of even width [25]. The extrapolated zero-temperature values for the  $S = 1$  chain,  $\chi_s(1, 0) = 18.6(1)$  and  $C_\pi(1, 0) = 3.83(2)$  agree well with the corresponding results of the exact diagonalization study by Sakai and Takahashi [36]. We also obtained

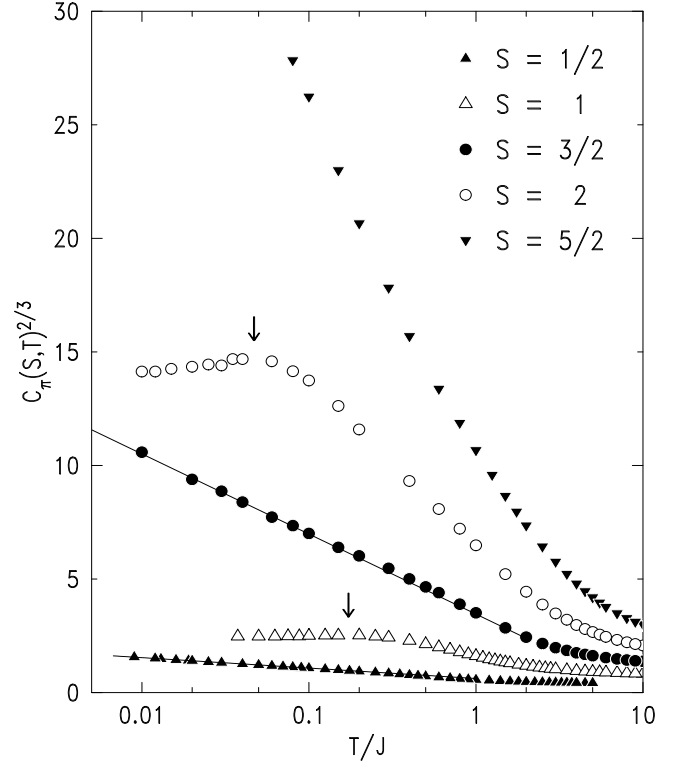


**Fig. 4.** Static structure factor peak intensity  $C_\pi(S, T)$  is plotted to show the linear dependence of  $C_\pi^{2/3}$  on  $\log T$ . The solid lines are fits to equation (9). The arrows indicate the peak positions as discussed in the text.

$\chi_s(2, 0) = 1160(10)$ , and  $C_\pi(2, 0) = 52.0(3)$  for the  $S = 2$  chain.

Recently, Starykh, Sandvik, and Singh [37] studied the static structure factor and the staggered susceptibility of the  $S = 1/2$  chain and obtained low-temperature analytic forms for these quantities:

$$\chi_s(S, T) = D_\chi(S) T^{-1} [\ln(T_\chi(S)/T)]^{1/2}, \quad (8)$$

$$C_\pi(S, T) = D_s(S) [\ln(T_s(S)/T)]^{3/2}. \quad (9)$$

We are able to fit our  $S = 1/2$  data to these forms and thereby to extract  $D_\chi(1/2) = 0.30(1)$ ,  $T_\chi(1/2) = 9.8(1.2)$ ,  $D_s(1/2) = 0.091(1)$ , and  $T_s(1/2) = 21(1)$ . The solid lines in Figures 3 and 4 are the results of fits to equations (8, 9) for  $T/J < 0.25$ . The parameters thus obtained agree with those of reference [37] to within 5%, except for  $T_\chi(1/2)$ . This is due to the difference in fitting range, since only very low temperature data show asymptotic behavior for  $\chi_s(S, T)$ . Our fitting range is  $0.009 \leq T/J < 0.25$ , while  $0.035 \leq T/J < 0.25$  was used in reference [37]. Our  $S = 3/2$  data can also be fitted to equations (8, 9) for  $T/J \leq 0.1$ . The parameters so-obtained are  $D_\chi(3/2) = 7.8(3)$ ,  $T_\chi(3/2) = 3.2(1.1)$ ,  $D_s(3/2) = 0.63(2)$ , and  $T_s(3/2) = 9.5(1.2)$ .

As shown in Figure 2, the correlation length in the spin-5/2 system TMMC is described well by the exact classical result. From equation (7) one sees that quantum effects only modify the classical behavior  $\xi \sim 1/T$

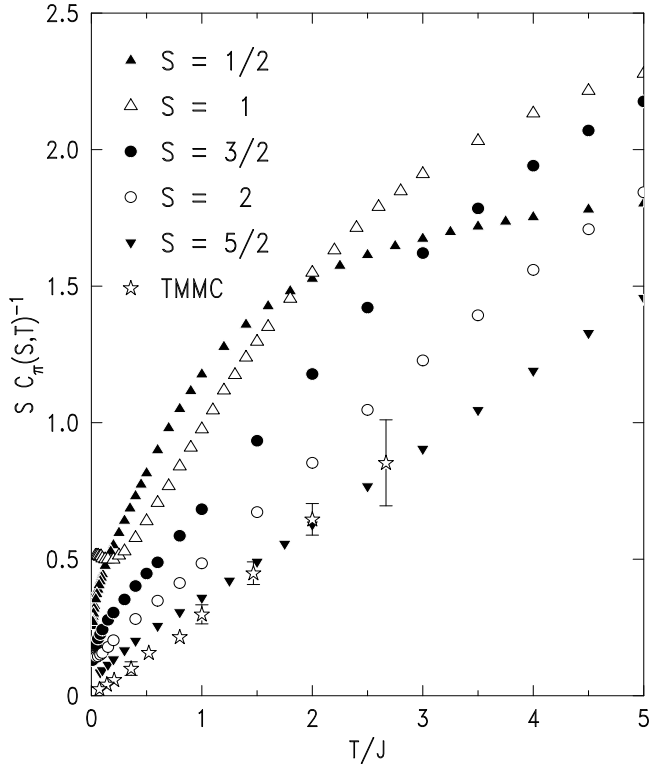


**Fig. 5.** Inverse static structure factor peak intensity  $C_\pi(S, T)^{-1}$ , multiplied by  $S$  for graphical purposes, versus  $T/J$ . Note the deviation of the quantum Monte-Carlo results for  $S = 5/2$  from the data for TMMC around  $T/J \sim 1$ .

by a logarithmic correction factor. On the other hand, for  $S = 1/2$  the structure factor in equation (9) changes from the classical form  $C_\pi(S, T) \sim 1/T$  to the quantum form  $C_\pi(S, T) \sim [\ln(T_s(S)/T)]^{3/2}$ ; this is a qualitative and not just a quantitative change due to quantum fluctuations in the divergence of  $C_\pi(S, T)$  with decreasing temperature. Assuming this also holds for  $S = 3/2$  and  $S = 5/2$ , we plot  $C_\pi(S, T)^{-1}$  versus  $T$  in Figure 5. It is evident that for  $S = 5/2$  there is a crossover from classical to quantum behavior around  $T/J \sim 1$ . Interestingly, the experimental data for TMMC do not seem to exhibit such a crossover. However, in TMMC there should also be a spin-space crossover from Heisenberg to  $XY$  behavior at the  $XY$  gap temperature, which is  $\Delta_{XY}/J \sim 0.7$ . In the  $XY$  regime,  $C_\pi(S, T)$  is enhanced. We speculate therefore that in TMMC the quantum and  $XY$  effects fortuitously cancel thus leading to the apparent classical  $1/T$  behavior observed down to very low temperatures. Future quantum Monte-Carlo calculations for  $S = 5/2$  including the  $XY$  anisotropy should serve to test this conjecture.

## 5 Discussion

In a recent theoretical study of gapped spin chains at non-zero temperature, Damle and Sachdev [27] developed a semiclassical picture based on thermally excited particles for  $T \ll \Delta$ . In this temperature regime, they were able

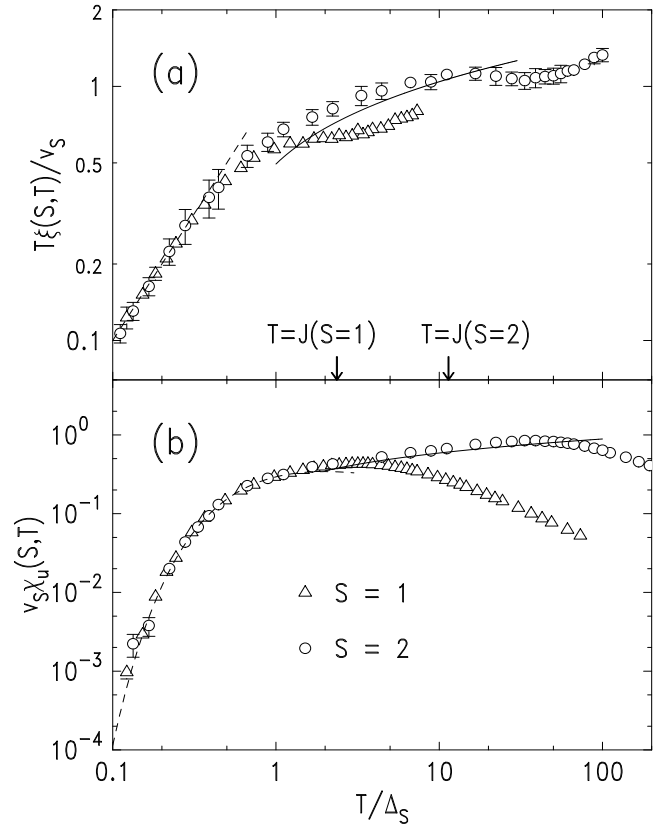


**Fig. 6.** (a) Correlation length and (b) uniform susceptibility as a function of temperature for integer spin chains. The solid lines are the results equations (10, 11) without any adjustable parameter. The dashed line in (a) is the relation  $v = \Delta\xi$ , and the dashed line in (b) is equation (4).

to obtain expressions for several dynamic properties of the  $O(3)$  nonlinear  $\sigma$  model. They also developed a rather different semiclassical approach for  $\Delta < T < J$  which is based upon classical waves described by the continuum  $O(3)$   $\sigma$  model. Using this approach, Damle and Sachdev derive one-loop expressions for the uniform susceptibility and correlation length in the temperature range  $\Delta < T < J$ :

$$\chi_u(S, T) = \frac{1}{3\pi v_S} \left[ \ln\left(\frac{32\pi T}{e^{\gamma+2}\Delta_S}\right) + \ln\ln\left(\frac{8T}{e\Delta_S}\right) \right] \quad (10)$$

$$\xi(S, T) = \frac{v_S}{2\pi T} \left[ \ln\left(\frac{32\pi T}{e^{\gamma+1}\Delta_S}\right) + \ln\ln\left(\frac{8T}{e\Delta_S}\right) \right], \quad (11)$$

where  $\gamma = 0.5772\dots$  is Euler's constant.

In Figure 6, we show  $T\xi(S, T)/v_S$  and  $v_S\chi_u(S, T)$  as functions of  $T/\Delta_S$  without any adjustable parameters, since  $\Delta_S$  and  $v_S$  have been determined independently. For the  $S = 1$  chain we use values  $\Delta_{S=1} = 0.41050(2)$ ,  $\xi(1, 0)/a = 6.03(1)$ , and  $v_{S=1}/Ja = 2.49(1)$  taken from the literature [29, 30], since these zero-temperature results have smaller error bars than our own values. The solid lines are equations (10, 11), which agree well with the  $S = 2$  data for  $\Delta_{S=2} < T < J$ . An even better agreement might be obtained if the theory were extended beyond the

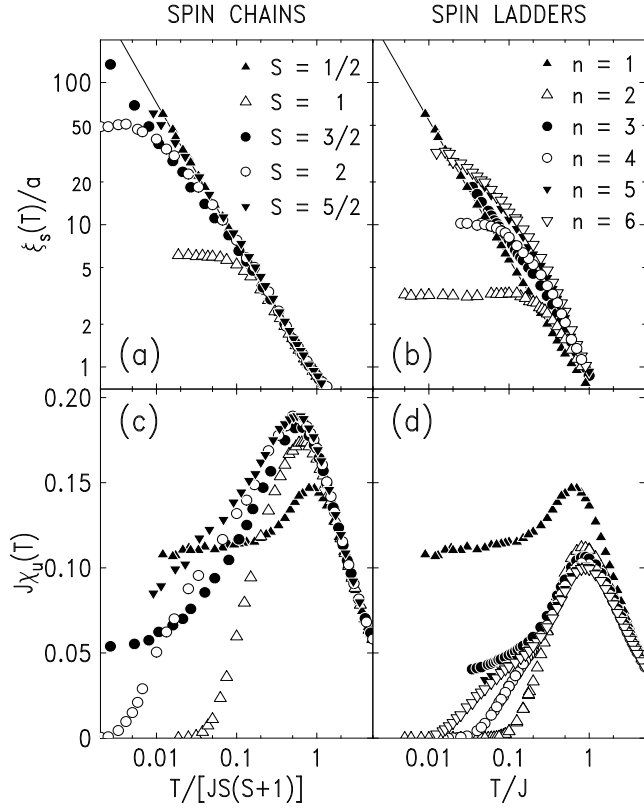


**Fig. 7.** Uniform susceptibility per spin and staggered correlation length of the quantum spin chains are compared with those of quantum spin ladders, consisting of  $n$  isotropically coupled antiferromagnetic  $S = 1/2$  chains [25]: (a) correlation length of spin chains; (b) correlation length of spin ladders; (c) uniform susceptibility of spin chains; and (d) uniform susceptibility of spin ladders. Solid lines in (a) and (b) are the WZNW model prediction, equation (7).

one-loop approximation. It is evident, nonetheless, that a window of temperature in which equations (10, 11) apply indeed exists for the  $S = 2$  chain, as speculated by Damle and Sachdev [27].

In Figure 6b, we also show the scaling of the uniform susceptibility at low temperatures ( $T \ll \Delta$ ) along with the theoretical expression equation (4) as a dashed line without any adjustable parameters. The dashed line in Figure 6a shows that the relation  $v = \Delta\xi$  holds up to  $T \approx \Delta/2$  in integer spin chains.

Spin-1/2 ladders are arrays of  $n$  coupled Heisenberg chains with  $S = 1/2$ . In analogy to integer spin chains, ladders with an even number  $n$  of chains exhibit exponentially decaying correlations in their ground state due to the presence of a spin gap, while those with odd  $n$  show behavior similar to that of half-odd-integer spin chains. Therefore, it is illuminating to plot the results such that the behaviors of quantum spin chains can be qualitatively compared with those of  $S = 1/2$  quantum spin ladders. In Figure 7, we display the staggered correlation length and the uniform susceptibility per spin for both spin chains and isotropically coupled spin ladders [25]. The same symbol is used for the spin- $S$  chain and the spin-1/2 ladder of

width  $n = 2S$ . One observes the markedly different behaviors of gapped systems shown in open symbols compared with those of gapless systems shown as solid symbols.

In summary, antiferromagnetic Heisenberg spin chains with spin values ranging from  $S = 1/2$  to  $S = 5/2$  have been studied with the quantum Monte-Carlo method. The temperature dependences of the uniform susceptibility, the staggered susceptibility, the static structure factor peak intensity, and the correlation length are obtained. We find that at high temperatures these quantities agree very well with the exact results for the classical spin chain, and that quantum effects become progressively more important as the temperature is decreased. In addition, our data for  $\chi_u$  and  $\xi$  for the  $S = 2$  chain in the intermediate temperature range  $\Delta_{S=2} < T < J$  are reasonably well predicted by the theory of Damle and Sachdev.

We would like to thank S. Sachdev and R.R.P. Singh for valuable discussions. This work was supported by the National Science Foundation-Low Temperature Physics Programs under award number DMR 97-04532 and by the International Joint Research Program of NEDO (New Economic Development Organization), Japan.

## References

1. R.J. Birgeneau, H.J. Guggenheim, G. Shirane, Phys. Rev. Lett. **22**, 720 (1969); Phys. Rev. B **1**, 2211 (1970).
2. R.J. Birgeneau, R. Dingle, M.T. Hutchings, G. Shirane, S.L. Holt, Phys. Rev. Lett. **26**, 718 (1971); M.T. Hutchings, G. Shirane, R.J. Birgeneau, S.L. Holt, Phys. Rev. B **5**, 1999 (1972)
3. For reviews, see R.J. Birgeneau, G. Shirane, Phys. Today **31**, 32 (1978); Physica B **86-88**, 639 (1977).
4. B. Keimer, N. Belk, R.J. Birgeneau, A. Cassanho, C.Y. Chen, M. Greven, M.A. Kastner, A. Aharony, Y. Endoh, R.W. Erwin, G. Shirane, Phys. Rev. B **46**, 14034 (1992); R.J. Birgeneau, A. Aharony, N.R. Belk, F.C. Chou, Y. Endoh, M. Greven, S. Hosoya, M.A. Kastner, C.H. Lee, Y.S. Lee, G. Shirane, S. Wakimoto, B.O. Wells, K. Yamada, J. Phys. Chem. Solids **56**, 1913 (1995).
5. M. Greven, R.J. Birgeneau, Y. Endoh, M.A. Kastner, M. Matsuda, G. Shirane, Z. Phys. B **96**, 465 (1995).
6. For a review, see E. Dagotto, T.M. Rice, Science **271**, 618 (1996).
7. H.G. Evertz, G. Lana, M. Marcu, Phys. Rev. Lett. **70**, 875 (1993); U.-J. Wiese, H.-P. Ying, Z. Phys. B **93**, 147 (1994); For a review, see H.G. Evertz, in *Numerical Methods for Lattice Many-Body Problems*, edited by D.J. Scalapino (Addison Wesley Longman, Reading, 1998).
8. T. Ami, M.K. Crawford, R.L. Harlow, Z.R. Wang, D.C. Johnston, Q. Huang, R.W. Erwin, Phys. Rev. B **51**, 5994 (1995); N. Motoyama, H. Esaki, S. Uchida, Phys. Rev. Lett. **76**, 3212 (1996).
9. D.C. Dender, P.R. Hammar, D.H. Reich, C. Broholm, G. Aeppli, Phys. Rev. Lett. **79**, 1750 (1997).
10. L.P. Regnault, I. Zaliznyak, J.P. Renard, C. Vettier, Phys. Rev. B **50**, 9174 (1994), and references therein.
11. J. Darriet, L.P. Regnault, Solid State Commun. **86**, 409 (1993).

12. H. Kadowaki, K. Hirakawa, K. Ubukoshi, J. Phys. Soc. Jpn **52**, 1799 (1983); S. Itoh, Y. Endoh, K. Kakurai, H. Tanaka, Phys. Rev. Lett. **74**, 2375 (1995).
13. G.E. Granroth, M.W. Meisel, M. Chaparala, T. Jolicœur, B.H. Ward, D.R. Talham, Phys. Rev. Lett. **77**, 1616 (1996).
14. H.A. Bethe, Z. Phys. **71**, 205 (1931).
15. J. des Cloizeaux, J.J. Pearson, Phys. Rev. **128**, 2131 (1962).
16. A. Luther, I. Peschel, Phys. Rev. B **9**, 2911 (1974).
17. F.D.M. Haldane, Phys. Lett. **93A**, 464 (1983).
18. M.P. Nightingale, H.W.J. Blöte, Phys. Rev. B **33**, 659 (1986).
19. J.P. Renard, M. Verdaguer, L.P. Regnault, W.A.C. Erkelens, J. Rossat-Mignod, W.G. Stirling, Europhys. Lett. **3**, 945 (1987).
20. S.P. Novikov, Sov. Math. Dokl. **24**, 222 (1981); Usp. Math. Nauk. **37**, 3 (1982); E. Witten, Commun. Math. Phys. **92**, 455 (1984).
21. T. Ziman, H.J. Schulz, Phys. Rev. Lett. **59**, 140 (1987).
22. For a review, see I. Affleck, J. Phys. Condens. Matter **1**, 3047 (1989).
23. M.E. Fisher, Am. J. Phys. **32**, 343 (1964).
24. H. Watanabe, Phys. Rev. B **50**, 13442 (1994).
25. M. Greven, R.J. Birgeneau, U.-J. Wiese, Phys. Rev. Lett. **77**, 1865 (1996); O.F. Syljuåsen, S. Chakravarty, M. Greven, Phys. Rev. Lett. **78**, 4115 (1997).
26. A.M. Tsvelik, Sov. Phys. JETP **66**, 221 (1987).
27. K. Damle, S. Sachdev, Phys. Rev. B **57**, 8307 (1998).
28. U. Schollwöck, T. Jolicœur, Europhys. Lett. **30**, 493 (1995); Phys. Rev. Lett. **77**, 2844 (1996); S. Yamamoto, Phys. Rev. Lett. **77**, 2845 (1996).
29. E.S. Sørensen, I. Affleck, Phys. Rev. B **49**, 15771 (1994).
30. S.R. White, D.A. Huse, Phys. Rev. B **48**, 3844 (1993).
31. B. Frischmuth, S. Hass, G. Sierra, T.M. Rice, Phys. Rev. B **55**, R3340 (1997), and references therein.
32. H.J. Schulz, Phys. Rev. B **34**, 6372 (1986), and references therein.
33. K. Hallberg, X.Q.G. Wang, P. Horsch, A. Moreo, Phys. Rev. Lett. **76**, 4955 (1996).
34. K. Nomura, Phys. Rev. B **40**, 2421 (1989).
35. K. Nomura, M. Yamada, Phys. Rev. B **43**, 8217 (1991).
36. T. Sakai, M. Takahashi, Phys. Rev. B **42**, 1090 (1990).
37. O.A. Starykh, A.W. Sandvik, R.R.P. Singh, Phys. Rev. B **55**, 14953 (1997).